Korean Journal of Remote Sensing, Vol.27, No.6, 2011, pp.653~662

Development of Land Surface Temperature Retrieval Algorithm from the MTSAT-2 Data

Ji-Hyun Kim and Myoung-Seok Suh †

Department of Atmospheric Science, Kongju National University, 182 Shinkwan-dong, Gongju-city 314-701, ChungCheongnam-do, Korea

Abstract : Land surface temperature (LST) is a one of the key variables of land surface which can be estimated from geostationary meteorological satellite. In this study, we have developed the three sets of LST retrieval algorithm from MTSAT-2 data through the radiative transfer simulations under various atmospheric profiles (TIGR data), satellite zenith angle, spectral emissivity, and surface lapse rate conditions using MODTRAN 4. The three LST algorithms are daytime, nighttime and total LST algorithms. The weighting method based on the solar zenith angle is developed for the consistent retrieval of LST at the early morning and evening time. The spectral emissivity of two thermal infrared channels is estimated by using vegetation coverage method with land cover map and 15-day normalized vegetation index data. In general, the three LST algorithms well estimated the LST without regard to the satellite zenith angle, water vapour amount, and surface lapse rate. However, the daytime LST algorithm shows a large bias especially for the warm LST (> 300 K) at day time conditions. The night LST algorithm shows a relatively large error for the LST (260 ~ 280K) at the night time conditions. The sensitivity analysis showed that the performance of weighting method is clearly improved regardless of the impacting conditions although the improvements of the weighted LST compared to the total LST are quite different according to the atmospheric and surface lapse rate conditions. The validation results of daytime (nighttime) LST with MODIS LST showed that the correlation coefficients, bias and RMSE are about 0.62~0.93 (0.44~0.83), -1.47~1.53 (-1.80~0.17), and 2.25~4.77 (2.15~ 4.27), respectively. However, the performance of daytime/nighttime LST algorithms is slightly degraded compared to that of the total LST algorithm.

Key Words : Land surface temperature, MTSAT-2, day & night LST algorithms

1. Introduction

In general, land-atmosphere interactions are mainly controlled by the biophysical parameters of land surface, such as the land surface temperature (LST), soil moisture, leaf area index, and roughness length. So, the LST is one of the key environmental variables which can be used in a wide range of applications, such as weather, climate modeling, hydrology, surface urban heat island and ecology (Prata and Cechet, 1999; Voogt and Oke, 2003; Hong *et al*., 2009a). However, LST is one of the most difficult

Received November 7, 2011; Revised November 30, 2011, Revised December 10, 2011; Accepted December 11, 2011.
† Corresponding Author: Myoung-Seok Suh (sms416@kongju.ac.kr)

surface variables to observe regularly due to the strong spatio-temporal variations. At present, the only available cost-effective operational systems capable of observing the LST at spatial and temporal resolutions appropriate to the various applications are the satellite sensors working in the thermal infrared and/or microwaves (Becker and Li, 1995; Peres and DaCamara, 2004).

After Becker and LI (1990) has retrieved the LST from meteorological satellite data by using split-window method, number of works have been performed to retrieve the LST from the satellite data, especially polar orbit satellites (Kerr *et al*., 1992; Ulivieri *et al*., 1994; Wan and Dozier, 1996; Sobrino and Romaguera, 2004; Suh *et al*., 2008; Hong *et al*., 2009a, b). However, operational retrieval of LST from the meteorological satellite data is very limited due to the poor quality of retrieved LST, especially by using geostationary satellite data over East Asia (Hong *et al*., 2009a). The combined effects of spectrally and temporally varying emissivity along with the atmospheric effects caused the poor quality of retrieved LST compared to that of sea surface temperature.

To retrieve the LST by using the split-window method from meteorological satellite data, spectral emissivity of land surface should be known as a function of time and location. The vegetation coverage method by using the normalized difference vegetation index (NDVI) derived from NOAA/AVHRR (Advanced Very High Resolution Radiometer) data is one of the widely used methods (Valor and Caselles, 1996; Jiang *et al*., 2006). The basic assumption of this method is that the pixel is mainly composed of temporally invariant soil and temporally varying vegetation. The temporal variation of vegetation can be obtained from the well known NDVI data. In this study, the land cover map of East Asian region classified by Kang *et al*.(2010) and MODIS (Moderate Resolution Imaging Spectroradiometer) NDVI are used for the retrieval of spectral emissivity of two thermal channels of MTSAT-2.

The strong merit of geostationary meteorological satellites is frequent observation (less than 30 minutes) for the given observing area. When we take into consider the strong temporal variability of LST, geostationary meteorological satellites (e.g., MSG/SEVIRI, MTSAT-1R, MTSAT2, COMS) are the most proper system for the regular monitoring of LST. The first operational retrieval of LST from geostationary meteorological satellite is performed by EUMETSAT LSA/SAF (Land Surface Analysis/Science Application Facility) (Peres and DaCamara, 2004; Sobrino and Romaguera, 2004).

Hong *et al*. (2009a) developed a split-window type LST algorithm by using MTSAT-1R data and evaluated the performance of LST algorithm using MODIS LST data. They showed that the LST over East Asia can be retrieved from MTSAT-1R data with the correlation coefficients and RMSE of about 0.82~0.99 and 1.5~4.28 K, respectively. However, the operation of MTSAT-1R is officially stopped on 31 June and MTSAT-2 observing images are operationally provided from 03 UTC on 1 July 2010. MTSAT-2, which sits in geostationary orbit at 145° E, has one visible and three infrared channels as well as MTSAT-1R. MTSAT-2 observes cloud and water-vapor distribution during the day and at night, as well as the temperature of the land surface, sea surface and cloud-tops. (http://mscweb.kishou.go.jp/operation/index.htm).

The goal of this study is to develop LST retrieval algorithm from MTSAT-2 data for the continuous retrieval of LST over East Asian region. The development of LST retrieval algorithm is explained in section 2. The sensitivity of LST retrieval algorithms to the various control factors, such as

emissivity and surface lapse rate, and validation results using MODIS LST are shown in section 3. The results are summarized in section 4.

2. Method

1) Radiative transfer model simulation

To retrieve the LST by using a split-window method, ground match-up data are needed for the coefficients of regression equation. However, unlike the sea surface temperature, available match-up data over East Asia are severely limited in LST. So, we performed radiative transfer model simulations (RTM) using MODTRAN4 with various atmospheric profiles, spectral emissivity and satellite zenith angle (SZA) as in Hong *et al*. (2009a, b). Thermodynamic Initial Guess Retrieval (TIGR2000) data sets were used as the atmospheric profiles for the radiative transfer simulations (http://ara.lmd. polytechnique. fr/htdocs-public/products/TIGR/ TIGR.html). Among the 2,311 atmospheric profile data sets, 535 profiles have been selected which have satellite viewing angles less than 60˚ from MTSAT-2 (points in the Fig. 1). The main differences between MTSAT1-R and MTSAT-2 are the location (MTSAT-1R: 140E, MTSAT-2: 145E) of satellite and spectral response

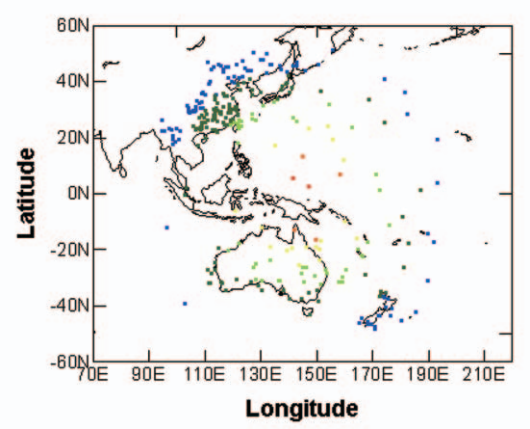

Fig. 1. Spatial distribution of TIGR data (points) used in this study.

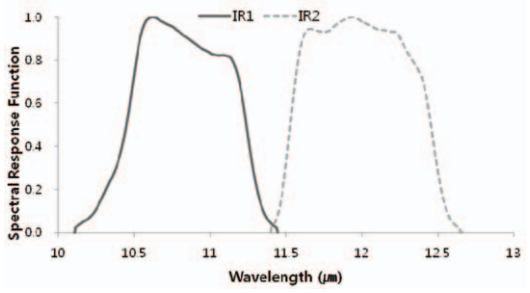

Fig. 2. Spectral response functions of two IR channels of MTSAT-2.

functions (see Fig. 2) of two IR channels. The atmospheric RTM simulations are designed to include all the impacting factors mentioned (Table 1).

2) Development of day and night LST

Table 1. Summary of atmospheric and surface conditions for the RTM simulations

Subject	Condition
Atmospheric profile	535 TIGR database (points in Fig. 1)
Satellite zenith angle	0˚ ~ 60˚
Land surface temperature	Total : T_a – 12K ~ T_a + 16K Day : T_a + 2K ~ T_a + 16K Night : T_a - 12K ~ T_a - 2K (interval: 2K)
Emissivity	ε_{IR1}: 0.9478~0.9968 (intv. : 0.0049) -0.02 $\leq \Delta\varepsilon \leq$ 0.012(intv. : 0.004) If $\varepsilon_{IR2} \geq$ 1.0 then ε_{IR2} = 0.9999

* **Total simulations:** 535(profiles) × 15(surface lapse rate) × 11(ε_{IR1}) × 9($\Delta\varepsilon$) = **794,475**
* Where, the T_a is the lowest layer air temperature in the TIGR data.

algorithms

Brightness temperature are produced by radiance generated through RTM simulation and MTSAT-2 spectral response functions (Fig. 2). In this study, we include the ΔT^2 to take into consider the nonlinear effect of water vapour. The LST retrieval algorithm has been developed by using a statistical regression method in the form of eq. (1).

$$LST = a + bT_{IR1} + c\Delta T + d\Delta T^2 + e(\sec\theta - 1) + f(1-\bar{\varepsilon}) + g\Delta\varepsilon \quad (1)$$

Where

T_{IR1} = Brightness temperature of IR1,

$\Delta T = T_{IR1} - T_{IR2}$(BTD),

θ = Satellite zenith angle,

$$\bar{\varepsilon} = \frac{\varepsilon_{IR1} + \varepsilon_{IR2}}{2}$$

$$\Delta\varepsilon = \varepsilon_{IR1} - \varepsilon_{IR2}$$

We have developed three sets of LST algorithm by using the total simulation, and day/night simulation data sets.

The derived coefficients for the three sets of LST algorithms are as follows:

$$LST_{tot} = 13.5345 + 0.948391T_{IR1} + 2.225\Delta T + 0.239163\Delta T^2 - 0.028085(\sec\theta - 1) + 53.5053(1-\bar{\varepsilon}) - 121.619\Delta\varepsilon \quad (2)$$

$$LST_{day} = 14.8721 + 0.94467T_{IR1} + 2.05229\Delta T + 0.251344\Delta T^2 - 0.66060(\sec\theta - 1) + 58.8353(1-\bar{\varepsilon}) - 138.867\Delta\varepsilon \quad (3)$$

$$LST_{ngt} = 20.1410 + 0.928570T_{IR1} + 1.92397\Delta T + 0.138161\Delta T^2 - 1.82487(\sec\theta - 1) + 42.8402(1-\bar{\varepsilon}) - 81.5052\Delta\varepsilon \quad (4)$$

3) Weighting technique for the consistent retrieval of LST

To retrieve the LST consistently with time during 24 hours, the LST of early morning and evening

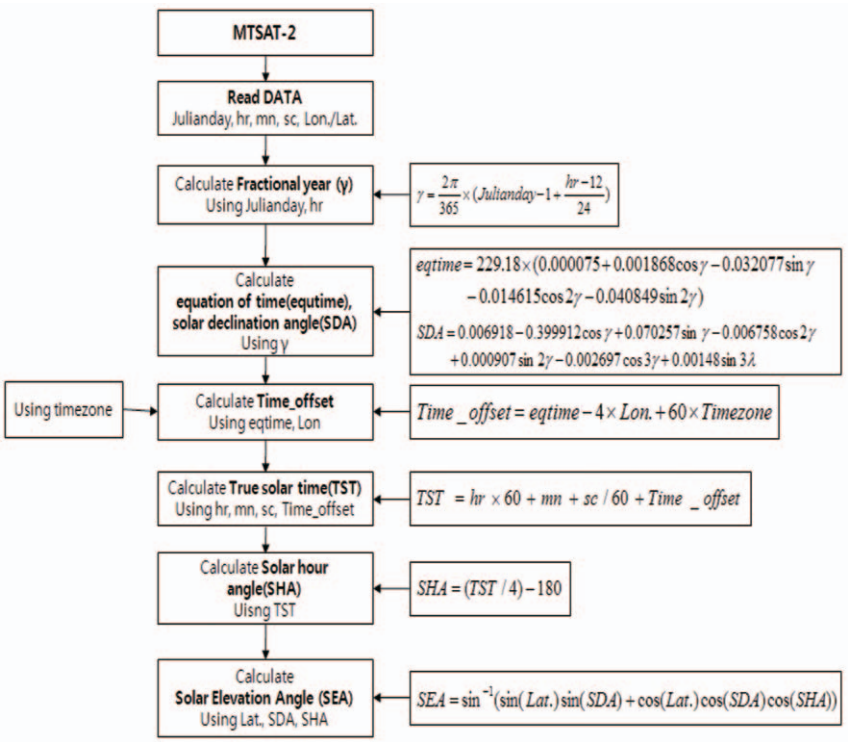

Fig. 3. Retrieval process of solar elevation angle for the decision of day and night conditions for the consistent LST retrieval from MTSAT-2 data.

should be calculated by using the weighed sum of LST_ngt and LST_day. The weighted mean of two LST is performed using eq. (5).

$$LST\_wgt = \omega \times LST\_ngt + (1-\omega) \times LST\_day \quad (5)$$

Where LST_ngt and LST_day represent the nighttime LST algorithm and daytime LST algorithm, respectively. And the ω is calculated as a function of local solar elevation angle (α) (Fig. 3).

$$\omega = \frac{1}{30}(\alpha + 15)\ (0 \le \omega \le 1) \quad (6)$$

The eq. (6) should be modified for the operational use based on the error analysis of retrieved LST for the various conditions.

3. Results

The performance of two LST algorithms, total and weighted sum of day/night algorithms, are investigated for the various impacting factors, such as atmospheric profiles (brightness temperature difference: BTD), $\Delta\varepsilon$, lapse rate at surface layer (Ts-Ta), satellite zenith angle, and more. To compare the relative performance of two LST algorithms (total: LST_tot and weighted sum: LST_wgt), bias and RMSE of two LST algorithms are analyzed.

Fig. 4 shows that theoretical performance of three sets of LST algorithm for the prescribed LST. The correlation and RMSE of three LST algorithms are larger and smaller than 0.98 and 2.0 K, respectively. In general, the retrieved LST shows a large bias for the warm LST (> 300 K) at day time conditions. Whereas, the retrieved LST shows a large bias for the normal LST (260 ~ 280K) at night time conditions.

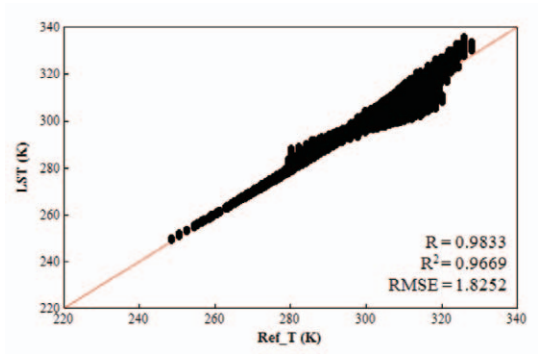

a) LST_tot

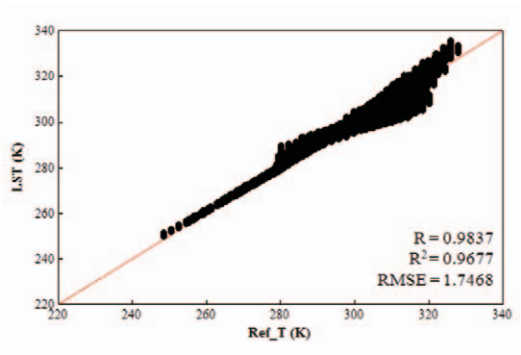

b) LST_day

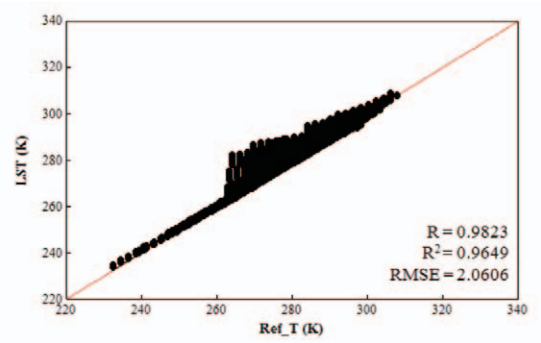

c) LST_tot

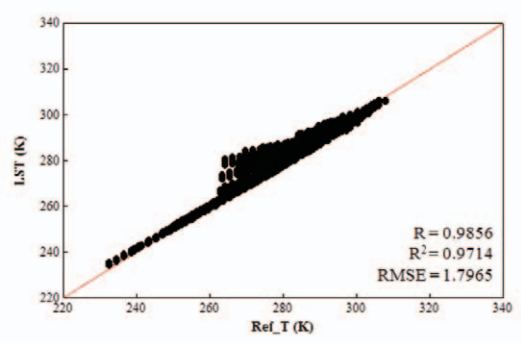

d) LST_ngt

Fig. 4. Scatter plots of retrieved LST (ordinate; LST) and prescribed LST (abscissa; Ref_T). a) and b) are for day condition (T_a+2K~T_a+16K). c) and d) are for night condition (T_a-12K~T_a-2K).

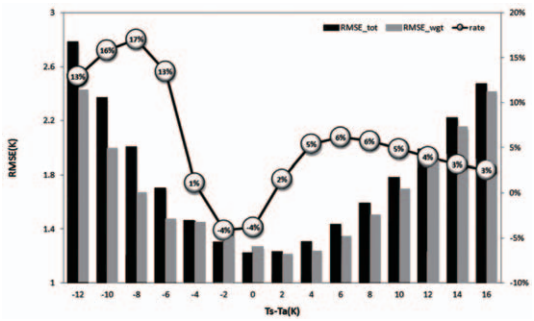

Fig. 5. Distribution of RMSE and the improvement rate in total and weighted LST algorithm according to the surface lapse rate (ΔT).

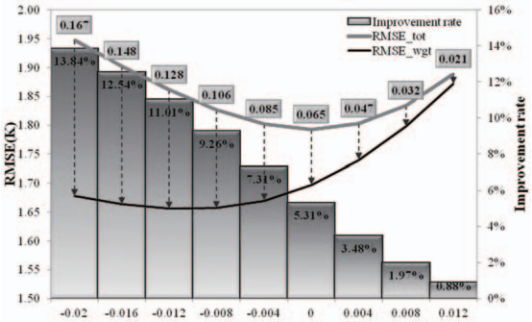

Fig. 6. Distribution of RMSE and the improvement ratio in LST_wgt algorithm according to $\Delta\varepsilon$.

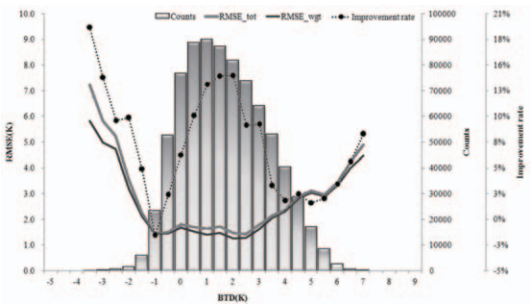

Fig. 7. Distribution of RMSE and improvement ratio of LST_wgt algorithm according to the BTD with the number of BTD data.

The improvement of day LST algorithm is relatively small compared to that of night LST algorithm. The large biases of three LST algorithms for the warm LST can be related with the nonlinear term, ΔT^2.

RMSE and the improvement rate in total and weighted LST algorithm according to the surface lapse rate (ΔT) are shown in Fig. 5. Two bars represent the RMSE of two LST algorithms and the line means the improvement ratio of weighted LST algorithm compared to the total LST algorithm. As shown in Fig. 5, the RMSE of two LST algorithms are clearly dependent on the surface lapse rate conditions, large at inversion (night time) and superadiabatic (afternoon) conditions and small at the neutral conditions. The RMSE of weighted mean LST is significantly decreased especially at the strong inversion conditions. However, the RMSE is slightly increased at the neutral conditions.

Fig. 6 shows that the RMSE of two LST algorithms and improvement ratio as a function of $\Delta\varepsilon$. The improvement rate (bars) is more significant when $\Delta\varepsilon$ is negative, the emissivity of 12 μm is larger than that of 11 μm.

The RMSE and improvement ratio in LST_wgt according to the BTD is shown in Fig. 7. The BTD ranges from -4K to 7K, most of them are located in -1K to +5K. The relatively large improvement in the LST_wgt for the small BTD means that the impact of surface lapse rate is relatively small when BTD is large. However, the RMSE is significantly large and improvement is small when the BTD is large, especially at the negative BTD. The large RMSE can be caused by the nonlinear the ΔT^2, in retrieval algorithm (Eq. (1)), over consideration of water vapour impact.

In order to validate the LST retrieved in this study, collocated MODIS LST data have been used. Because the pixel size of MODIS is 1 km, the MODIS data are averaged in 4 x 4 pixels for the same size of MTSAT-2 pixel. The criterion for cloudy or clear was based on the MODIS data, so the cloudy pixels in the MODIS LST data were excluded from the averages. The exact time of overpass for each image was calculated, because temporal variation of

LST is very significant, especially during the daytime under dry conditions, and images with differences of less than ±15 minutes were selected. Although the ± 15 minutes are not a short time for LST comparison, particularly for daytime, we used this threshold to allow for the acquisition of more validation samples.

Fig. 8 shows a spatial distribution of LST differences between LST from MTSAT-2 and LST from MODIS over the Korean peninsula at nighttime and daytime. The white indicates the pixels covered by clouds. The LST differences between MODIS and MTSAT-2 are clearly different from day to night. In general, the LST retrieved in this study are warmer and colder than the MODIS LST at daytime and nighttime without regard to the retrieval methods, respectively. The warm and cold biases of daytime and nighttime LST algorithms are +3~4K and -1~3K, respectively. The different bias patterns between day and night can be caused by the non-linear terms (△T2) in the retrieval algorithms (e.g., Eq. (4)). More studies are needed for the detailed causes of the different bias patterns between day and night. However, the differences between day/nighttime and total LST are less than ±1 without regard to the geographic location and retrieval time. It means that the impacts of surface layer conditions on the LST retrieval are not significant at this case. So, more cases study is needed for the operational use of day/night algorithm instead of the total LST algorithm.

Statistical validation results for the selected daytime and nighttime cases are shown in Table 2

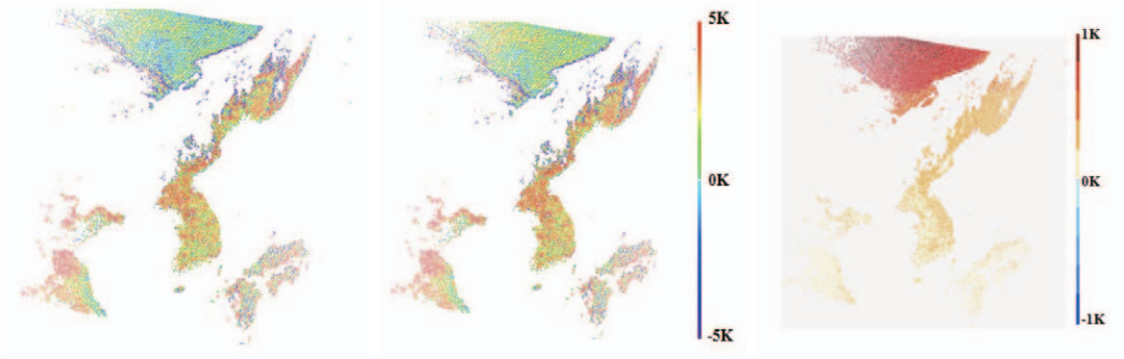

a) LST_tot - MODIS b) LST_day - MODIS c) LST_day - LST_tot

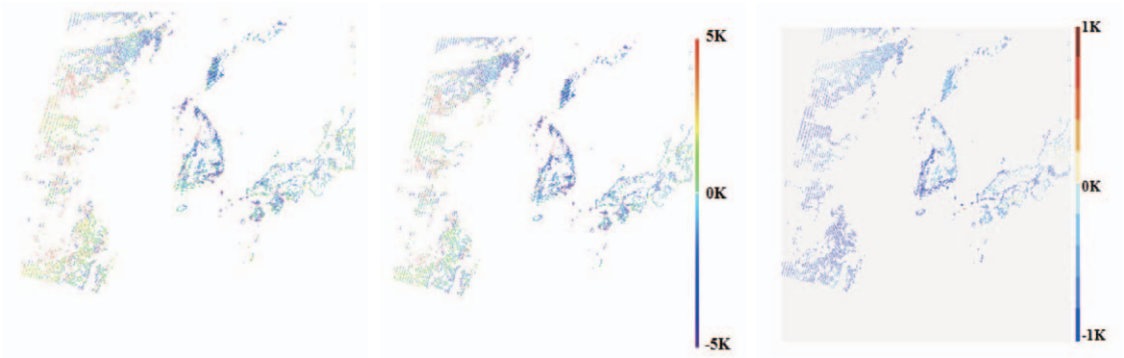

d) LST_tot - MODIS e) LST_ngt - MODIS f) LST_ngt - LST_tot

Fig. 8. Spatial distribution of differences between MTSAT-2 LST and MODIS LST. a), b), and c) are day case (0233 UTC 16 Sept. 2010). d), e), and f) are night cases (1715UTC 04 Sept. 2010).

Table 2. Validation results of daytime MTSAT-2 LST by using Terra/MODIS LST

Time		LST_tot		LST_day			
MTSAT-2 (mmdd - UTC)	MODIS (mmdd - UTC)	R	Bias(K)	RMSE(K)	R	Bias(K)	RMSE(K)
0809 - 0300	0809 - 0305	0.622	1.057	3.868	0.623	1.159	3.856
0821 - 0200	0821 - 0150	0.640	1.774	4.281	0.640	1.877	4.281
0904 - 0200	0904 - 0200	0.839	1.537	4.772	0.837	1.732	4.818
0916 - 0233	0916 - 0225	0.890	1.290	3.436	0.887	1.707	3.552
1010 - 0133	1010 - 0135	0.758	-1.476	3.366	0.747	-0.962	3.242
1018 - 0233	1018 - 0225	0.933	1.313	2.256	0.932	1.994	2.741
Ave.		**0.780**	**0.916**	**3.663**	**0.778**	**1.251**	**3.748**

Table 3. Same as in Table 2 except for the Aqua/MODIS

Time		LST_tot		LST_day			
MTSAT-2 (mmdd - UTC)	MODIS (mmdd - UTC)	R	Bias(K)	RMSE(K)	R	Bias(K)	RMSE(K)
0706_1833	0706_1840	0.443	-1.800	4.279	0.418	-3.252	4.952
0803_1715	0803_1720	0.829	-0.031	2.865	0.846	-0.902	2.720
0809_1833	0809_1825	0.819	0.172	2.158	0.823	-1.075	2.241
0904_1715	0904_1720	0.834	-0.722	2.988	0.842	-1.365	3.065
Ave.		**0.731**	**-0.595**	**3.073**	**0.732**	**-1.649**	**3.245**

and Table 3. In general, the performance of night LST algorithm is superior in every assessment measure to that of daytime. The validation results of daytime (nighttime) LST with MODIS LST showed that the correlation coefficients, bias and RMSE are about 0.62~0.93 (0.44~0.83), -1.47~1.53 (-1.80 ~ 0.17), and 2.25~4.77 (2.15 ~ 4.27), respectively. However, the performance of daytime/nighttime LST algorithms are slightly degraded compared to that of the total LST algorithm as shown in Fig. 8. The large variations of LST retrieval results day by day are mainly caused by the different environment of LST retrieval location, such as land cover, soil moisture and viewing geometry. The impact of soil moisture on the emissivity is not included in this study.

4. Summary

In this study, we have developed the three sets of LST retrieval algorithms from MTSAT-2 data through the radiative transfer simulations under various atmospheric profiles (TIGR data), satellite zenith angle (SZA), spectral emissivity, and surface lapse rate conditions using MODTRAN 4. We have developed daytime and nighttime LST algorithms separately by using the different match-up data base according to the surface lapse rate conditions to improve the quality of retrieved LST. The final LST (LST_wgt) is recalculated by using weighted mean of the two LST (LST_day and LST_ngt) for the consistent retrieval of LST at the early morning and evening time based on the solar zenith angle.

In general, the daytime LST algorithm shows large biases for the warm LST (> 300 K) at day time conditions. Whereas, the night LST algorithm shows relatively large biases for the normal LST (260 ~ 280K) at night time conditions. Although the improvements in LST_wgt are quite different according to the atmospheric and surface lapse rate

conditions, the performance of LST_wgt is clearly improved regardless of the impacting conditions in the sensitivity analysis.

The validation results of daytime (nighttime) LST with MODIS LST showed that the correlation coefficients, bias and RMSE are about 0.62~0.93 (0.44~0.83), -1.47~1.53 (-1.80~0.17), and 2.25~4.77 (2.15~4.27), respectively. However, the performance of daytime/nighttime LST algorithms is slightly degraded compared to that of the total LST algorithm. Prata and Cechet (1999) mentioned that accuracies of 3 K (RMSE of LST) are of marginal use, while accuracies of 1 K are potentially of great benefit in many applications. Although the MODIS LST is not perfect ground-truth data, the correlation coefficients, bias, and RMSE showed that the LST-retrieval algorithm developed in this study can be used for LST retrieval in this region.

Acknowledgements

This research was supported by the project: The Korea Meteorological Administration Research and Development Program under Grant CATER 2009-3114.

References

Becker, F., and Z.L. Li, 1990. Toward a local split window method over land surface, *International Journal of Remote Sensing*, 3: 369-393.

Becker, F. and Z.-L. Li, 1995. Surface temperature and emissivity at various scales: Definition, measurement and related problems, *Remote Sensing Reviews*, 12: 225-253.

Han, K.-S., A.A. Viau, and F. Anctil, 2004. An analysis of GOES and NOAA derived land surface temperatures estimated over a boreal forest, *International Journal of Remote Sensing*, 25: 4761-4780.

Hong, K.O., M.S. Suh, and J.H. Kang, 2009a. Development of a Land Surface Temperature retrieval Algorithm from MTSAT-1R data, *Asia-Pacific Journal of Atmospheric Sciences*, 45(3): 412-421.

Hong, K.O., M.S. Suh, and J.H. Kang, 2009b. Improvement of COMS Land Surface Temperature Retrieval Algorithm, *Korean Journal of Remote Sensing*, 25(6): 1-10.

Jiang, J-M., Z.-L. Li, and F. Nerry, 2006. Land surface emissivity retrieval from combined mid-infrared and thermal infrared data of MSG-SEVIRI, *Remote Sensing of the Environment*, 105: 326-340.

Kang, J.-H., M.-S. Suh, and C.-H., Kwak, 2010. Land cover classification over East Asian region using recent MODIS data (2006-2008). *Atmosphere*, 20: 415-426.

Kerr, Y.H., J.P. Lagouarde, and J. Imbernon, 1992. Accurate land surface temperature retrieval from AVHRR data with use of an improved split window, *Remote Sensing of the Environment*, 41: 197-209.

Peres L. and C.C. DaCamara, 2004. Land surface temperature and emissivity estimation based on the two-temperature method: sensitivity analysis using simulated MSG/SEVIRI data, *Remote Sensing of the Environment*, 91: 377-389.

Prata, A.J. and R.P. Cechet, 1999. An assessment of the accuracy of land surface temperature determination from the GMS-5 VISSR, *Remote Sensing of the Environment*, 67: 1-14.

Price, J.C., 1984. Land surface temperature measurements from the split-window channels of the NOAA 7 AVHRR, *Journal of*

Geophysical Research, 89: 7231-7237.

Sobrino, J.A. and M. Romaguera, 2004. Land surface temperature retrieval from MSG1-SEVIRI data, *Remote Sensing of the Environment*, 92: 247-254.

Suh, M.-S., S.-H. Kim, and J.-H. Kang, 2008. A comparative study of algorithms for estimating land surface temperature from MODIS data, *Korean Journal of Remote Sensing*, 24: 65-78.

Ulivieri, C., M.M. Castronouvo, R. Francioni, and A. Cardillo, 1994. A split-window algorithm for estimating land surface temperature from Korean Journal of Remote Sensing, Vol.25, No.6, 2009-8 satellites, *Advances in Space Research*, 14: 59-65.

Valor, E. and V. Caselles, 1996. Mapping land surface emissivity from NDVI: Application to European, African, and South American areas, *Remote Sensing of the Environment*, 57: 164-184.

Voogt, J.A. and T.R. Oke, 2003. Thermal remote sensing of urban climates, *Remote Sensing of Environment*, 86:370-384.

Wan Z. and J. Dozier, 1996. A generalized split window algorithm for retrieval of land surface temperature from space, *IEEE Transactions on Geoscience and Remote Sensing*, 34: 892-905.